



Identification of pivotal genes with prognostic evaluation value in lung adenocarcinoma by bioinformatics analysis

Yushan Wang^{1,2}, Ruihong Wang³, Ji Ma³, Tingting Wang⁵, Cuiping Ma⁴, Yuchao Gu^{1,2}, Yanxia Xu^{3,*}, Ye Wang^{5,*}

¹School of Medicine and Pharmacy, Ocean University of China, Qingdao 266003, China

²Key Laboratory of Marine Drugs, Ministry of Education, Qingdao 266003, China

³Department of Combine Traditional Chinese and Western Medicine, Affiliated Qingdao Central Hospital of Qingdao University, Qingdao Cancer Hospital, Qingdao, 266042, China

⁴Shandong Provincial Key Laboratory of Biochemical Engineering, Qingdao Nucleic Acid Rapid Detection Engineering Research Center, College of Marine Science and Biological Engineering, Qingdao University of Science and Technology, Qingdao, 266042, China

⁵Core Laboratory, The Affiliated Qingdao Central Hospital of Qingdao University, Qingdao, 266042, China

ARTICLE INFO

Original paper

Article history:

Received: June 03, 2023

Accepted: August 22, 2023

Published: August 31, 2023

Keywords:

lung adenocarcinoma, prognosis, bioinformatics, TCGA, cancer

ABSTRACT

Lung cancer remains the leading cause of cancer morbidity and mortality worldwide, and over-diagnosis causes various unnecessary losses in patients' lives and health. How to more effectively screen lung cancer patients and their potential prognostic risk become the focus of our current study. By analyzing the LUAD expression profile in The Cancer Genome Atlas (TCGA), we constructed a weighted gene co-expression network using differentially expressed genes (DEGs) to find the key modules and pivotal genes. A COX proportional risk regression model based on the least absolute shrinkage and selection operator (LASSO) was used to assess the predictive value of the model for the prognosis of LUAD patients. A total of 4107 up-regulated DEGs and 2022 down-regulated DEGs were identified in this study, and enrichment analysis showed that these analyzes were associated with the extracellular matrix of cells and adhesion. Ten gene markers consisting of LDHA, TOP2A, UBE2C, TYMS, TRIP13, EXO1, TTK, TPX2, ZWINT, and UHRF1 were established by extracting the central genes in the key modules, and the upregulation of these genes was accompanied by an increased prognostic risk of patients. Among them, high expression of LDHA, TRIP13, and TTK in LUAD was associated with shorter overall survival and could be used as independent prognostic factors to participate in metabolic processes such as tumor NAD. The present study provides a powerful molecular target for the study of LUAD prognosis and provides a theoretical basis for the diagnosis and treatment of LUAD and the development of targeted inhibitors.

Doi: <http://dx.doi.org/10.14715/cmb/2023.69.8.34>

Copyright: © 2023 by the C.M.B. Association. All rights reserved.

Introduction

Lung cancer continues to lead the list of cancers in terms of incidence and mortality, posing a serious burden on global public health and continues to increase year by year with increased industrialization and increased use of medicinal herbs worldwide (1,2). As a major cause of cancer death, imaging technologies such as computed tomography have effectively reduced the mortality rate of lung cancer patients but also forced patients to face various side effects such as long-term radiotherapy and false-positive diagnosis, and overdiagnosis is a potential risk factor in lung cancer diagnosis and treatment (3), in order to avoid unnecessary losses in patients' lives and finances, we need to explore more In order to avoid unnecessary losses in patients' lives and finances, we need to explore more reliable treatment mechanisms to protect the prognosis of patients.

The most important hallmark of modern medicine in the century is the rewriting of the biological map of cancer. The arrival of biological markers of cancer has provided a more personalized approach to patient treatment, making the malignant transformation of cancer more traceable and enabling new strategies of human defense against cancer,

such as immune blockade and radiobiology (4). Lung adenocarcinoma (LUAD), the most common and most diagnosed type of lung cancer, is mainly caused by aberrant alterations in a single oncogenic factor and is frequently reported regarding the activation and overexpression of certain specific oncogenes in its tumor cells, which seem to constitute the main oncogenic mechanism of lung cancer (5). The improvement of technologies such as high-throughput sequencing provides powerful technical support for the screening of key candidate genes in LUAD, providing new access to information for the exploration of "addictive" oncogenes in LUAD and a broader prospect for the development of new biological markers and their corresponding new drugs (6).

In this study, we collected expression data from The Cancer Genome Atlas (TCGA) of 513 tumor samples of LUAD and 59 corresponding normal samples, screened the differentially expressed genes (DEGs), and constructed a weighted gene co-expression network analysis (WGCNA) to find the most relevant gene modules of LUAD and pivotal genes among them, to provide new biological markers for predicting prognosis of LUAD patients.

* Corresponding author. Email: xyx1021@126.com; yewang@qdu.edu.cn

Materials and Methods

Data download and analysis of variance

The expression profiles and clinical information of LUAD patients were collected from the TCGA (<https://portal.gdc.cancer.gov/>) database. A total of 513 tumor samples and 59 normal samples were included. DEGs were screened according to gene counts using the R package edgeR. The screening criteria were $|\log_2(\text{FC})| > 1$ and $P\text{Value} < 0.05$. The visualization was performed using the R package ggplot2.

Functional enrichment analysis

Gene ontology (Go) enrichment analysis of DEGs was performed using the R package cluster profile to illustrate the biological functions of DEGs in terms of biological processes (BP), cellular components (CC), and molecular functions (MF). In addition, the gene data set h.all.v7.1.symbols.GMT was downloaded from the Gene Set Enrichment Analysis (GSEA) database (<https://www.gsea-msigdb.org/gsea/index.jsp>), and GSEA was performed between tumor tissues and normal samples by using the tool GSEA, based on $\text{FDR} < 25\%$, $p < 0.05$ screened for significantly enriched encyclopedia (KEGG) gene sets.

Weighted gene co-expression network analysis (WGCNA)

Co-expression networks were constructed and modules were identified using the R package WGCNA, normalized against sample depth based on $\log(\text{cpm}+1)$, and log-transformed. A soft threshold power $\beta=6$ is set according to the scale-free topology criterion, the adjacency matrix is converted into a topological overlap matrix (TOM), and the average link hierarchical clustering is performed based on the TOM dissimilarity (1-TOM) metric. The modules were cut and identified according to the dynamic tree, and the genes with similar expression profiles were clustered, where the minimum number of genes in the modules was 30, and the cut height was set to 0.3, and the modules with the height of the module feature gene (ME) lower than 0.25 were merged.

Screening of pivotal genes

Scatter plots of correlations between module gene membership (MM) and gene salience (GS) were plotted to assess gene connectivity within modules. Genes in key modules were imported into the STRING database to identify protein-protein interaction networks (PPIs), visualize PPIs using Cytoscape software (version 3.8.2) (<https://cytoscape.org/download.html>), and use the Maximal Clique Centrality (MCC) algorithm to screen pivotal genes.

Survival analysis

The prognostic characteristics of pivotal genes were first elucidated using COX proportional risk regression analysis, followed by the least absolute shrinkage and selection operator (LASSO) model using the R package glmnet and survival, where the risk score was the sum of the products of gene expression and Coef coefficients, and patients were classified into low and high-risk groups based on the median risk score. The risk score prediction model for patient prognosis was validated by plotting risk factor linkage using the R package ggplot2 and plotting subject operating characteristic curves (ROC) and Kaplan-

Meier survival curves. Finally, by using the function surv_cutpoint in the R package survminer, the best separation cut-off was classified according to the FPKM to determine the high and low mRNA expression of the target gene and survival curves were plotted to classify the high and low expression.

Results

Screening and functional enrichment of DEGs

Differential analysis showed that 4107 genes were up-regulated and 2022 genes were downregulated in LUAD tumor tissues compared with normal tissues (Figure 1A). GO enrichment analysis showed that overlapping DEGs were mainly enriched in the extracellular matrix, extracellular structures, intercellular adhesion, and cAMP-mediated signaling (Figure 1B). GSEA showed that tumor samples with DEGs were associated with signaling pathways such as Nod-like receptor, and Toll-like receptor (Figure 1C).

Construction of co-expression modules

Genes with similar expression patterns in DEGs were clustered and characterized by constructing co-expression modules (Figure 2A), and a total of 26 gene modules were identified (Figure 2B). As seen in Figure 3C, turquoise module members were relatively highly correlated with tumors (coefficient = 0.54, $P < 0.001$), so the turquoise module was selected as the key module.

Screening and identification of pivotal genes

The scatter plot of MM and GS correlations in the turquoise module (Figure 3A) revealed that DEG, which was significantly associated with Cancer status, was also an important gene member in the turquoise module ($\text{cor}=0.45$, $P < 0.001$). PPI was constructed based on the STRING database, and a total of 187 points and 1287 edges were identified (Figure 3B). The MCC algorithm using CytoHubba plug-in in Cytoscape software was used for pivotal gene screening, in which the top 10 genes with the highest MCC scores were designated as pivotal genes: LDHA, TOP2A,

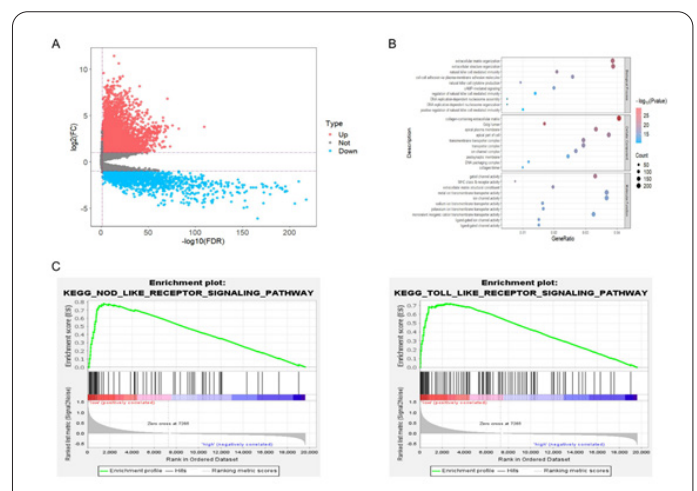


Figure 1. RNA-Seq differential expression and functional enrichment analysis in LUAD tumor samples and normal samples. (A) volcano plot of DEGs, blue is down-regulated, red is up-regulated, LUAD: lung adenocarcinoma, DEGs: differentially expressed genes; (B) top 10 GO terms, GO: gene ontology, BP: biological process, MF: molecular function; (C) enrichment plot of GSEA, KEGG: an encyclopedia.

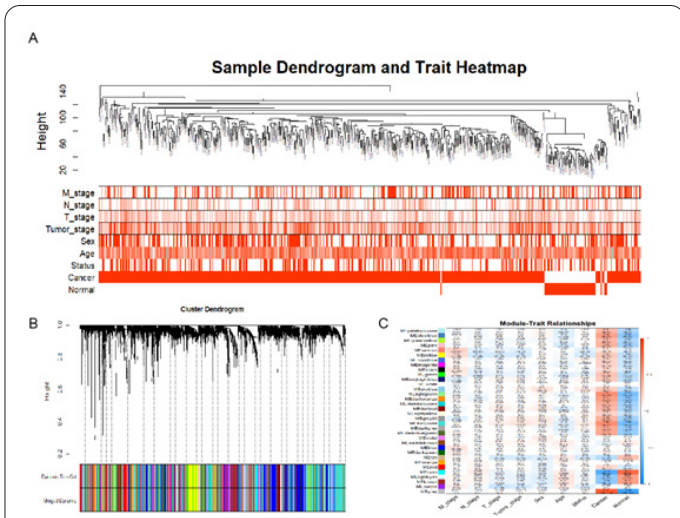


Figure 2. Identification of co-expression network modules. (A) Clustering dendrogram of samples and heat map of clinical characteristics, based on the expression matrix of tumor samples and normal samples DEGs from LUAD for clustering, including color intensity positively correlated with T_stage, M_stage, N_stage, Tumor_Stage, Sex, Age, except that white represents female, surviving or normal samples, red represents male, death or tumor samples, and gray indicates absence. (B) DEGs clustering dendrogram based on the phase dissimilarity measure (1-TOM), TOM: topological overlap matrix; (C) Heat map of correlation between module feature genes and clinical features.

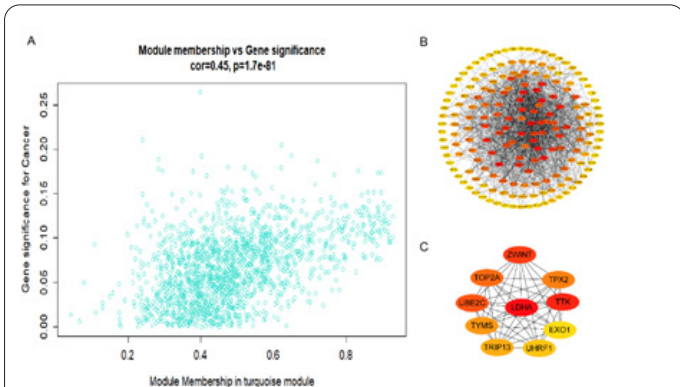


Figure 3. Screening of pivotal genes. (A) Correlation between module gene members and gene significance in the turquoise module; (B) Protein-protein interaction network (PPI) of 187 overlapping genes was constructed by Cytoscape software; (C) Top 10 pivotal genes with the highest MCC scores.

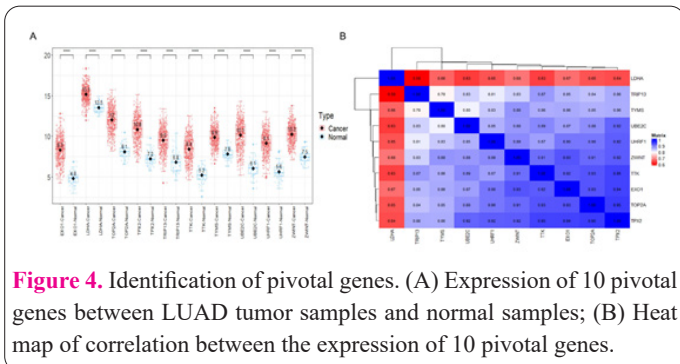


Figure 4. Identification of pivotal genes. (A) Expression of 10 pivotal genes between LUAD tumor samples and normal samples; (B) Heat map of correlation between the expression of 10 pivotal genes.

UBE2C, TYMS, TRIP13, EXO1, TTK, TPX2, ZWINT, UHRF1 (Figure 3C). By comparing the gene expression of genes between tumor samples and normal samples, we found that all of these 10 genes were up-regulated in the LUAD tumor samples (Figure 4A). As shown in Figure 4B, the correlation between the expression of LDHA and

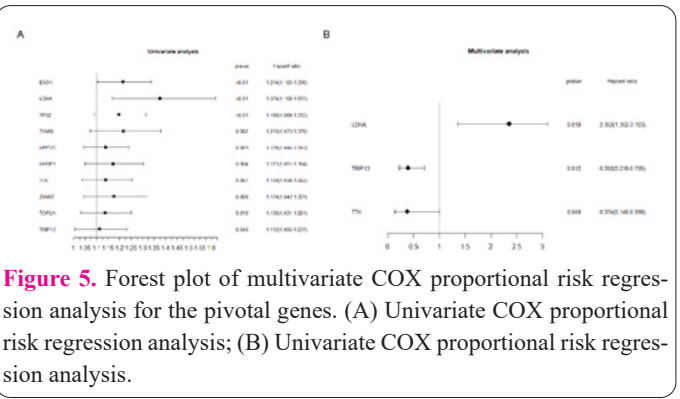


Figure 5. Forest plot of multivariate COX proportional risk regression analysis for the pivotal genes. (A) Univariate COX proportional risk regression analysis; (B) Univariate COX proportional risk regression analysis.

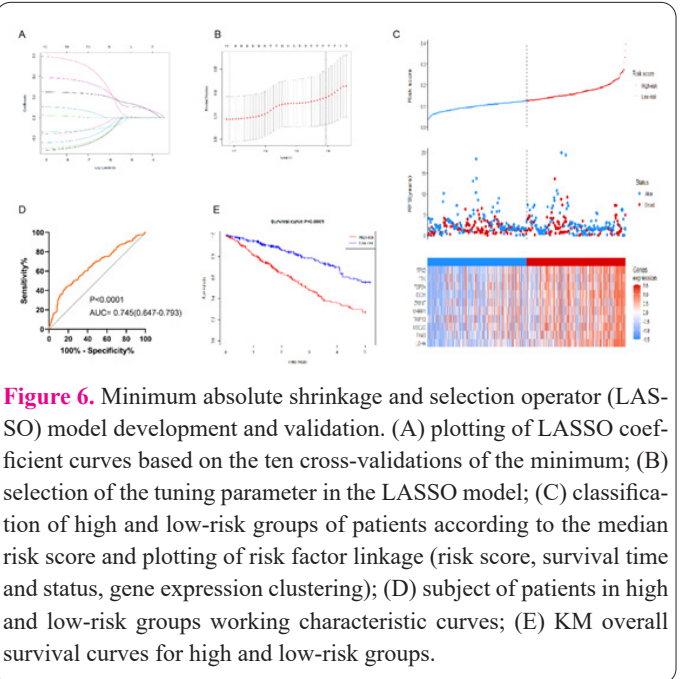


Figure 6. Minimum absolute shrinkage and selection operator (LASSO) model development and validation. (A) plotting of LASSO coefficient curves based on the ten cross-validations of the minimum; (B) selection of the tuning parameter in the LASSO model; (C) classification of high and low-risk groups of patients according to the median risk score and plotting of risk factor linkage (risk score, survival time and status, gene expression clustering); (D) subject of patients in high and low-risk groups working characteristic curves; (E) KM overall survival curves for high and low-risk groups.

the other 9 genes was weak.

Prognostic ability and functional analysis of pivotal genes

The best model to predict the prognosis of LUAD patients was determined by univariate COX proportional risk regression analysis, which revealed an association between the expression levels of all 10 pivotal genes and the overall survival of patients (Figure 5A), followed by the identification of three independent prognostic factors (LDHA, TRIP13, TTK) based on multifactorial COX proportional risk regression analysis (Figure 5B).

Meanwhile, we ran cross-validation to construct the LASSO model by analyzing the trajectories of each independent variable (Figure 6A-B). As shown in Figure 6C, patients in the high-risk group had a higher risk of survival, and the ROC confirmed the accuracy of the prognostic risk score prediction (Figure 6D), and the results of the Kaplan-Meier analysis also indicated that low-risk patients had a better prognosis than high-risk patients (Figure 6E).

Finally, we compared the survival of patients with high and low expression of LDHA, TRIP13, and TTK by plotting Kaplan-Meier survival curves, and patients with high expression of these three key genes had a worse prognosis than their respective low expression (Figure 7), indicating that the expression levels of these three key genes were closely related to the prognosis of LUAD patients. GO analysis also showed that these three genes are associated with cancer-related processes such as NAD metabolism,

and para-cAMP, and are involved in signaling pathways such as pyruvate metabolism and HIF-1 (Figure 8).

Discussion

Since the joint launch of the TCGA project by the National Cancer Institute and the National Institute of Human Genetics in 2006, a steady influx of 33 cancer cases in humans has been added to the TCGA database, and the richness and size of the TCGA dataset have helped one to define human cancers more meaningfully (7). By analyzing and comparing the altered genetic signatures in TCGA tumor samples, key genes that drive altered tumor patterns in a targeted manner can be obtained, and targeting these drivers can effectively improve clinical treatment planning and reduce vulnerability in treatment selection, providing an opportunity to improve targeted sniping in cancer treatment (7,8).

In our current study, we found 6129 DEGs in 513 tumor samples and 59 normal samples from LUAD by differential analysis, and these genes were commonly associated with the extracellular matrix, intercellular adhesion, cAMP signaling, and other BPs that affect cell migration ability (9), and altering matrix arrangement and coordinating intercellular adhesion are targeted cell invasion ability in cancer treatment important targets for preventing distant metastasis of cancer cells and improving chemotherapy efficacy (10-12). GSEA is a governing method to gain insight into the biological characterization of gene sets (13), and our current analysis by GSEA revealed that genes upregulated in LUAD tumor tissues are significantly enriched in relevant pathways in inflammatory cancer transition, and these signaling pathways are often in maintaining the dynamic homeostasis of tissues have a crucial role, and targeting these signaling could provide potential alternative therapies for tumor treatment (14-17).

Since WGCNA can identify correlations between gene pairs and group them (18,19), WGCNA is now widely used to find modules and hub genes associated with specific traits (20,21). This time, we focused on the DEGs in LUAD samples, and a total of 26 different color modules were classified. Among them, the turquoise module has a relatively high correlation with tumors. The high correlation between MM and GS in a turquoise module indicates that the gene members of a turquoise module are closely related to LUAD status. And by calculating the MCC scores, we found that all of the top 10 genes centrally linked to PPI were upregulated in tumor samples with LUAD and high expression levels suggesting poor patient prognosis.

LASSO COX is a powerful survival prediction model commonly used to identify prognostic factors associated with cancer risk and is able to treat all genes equally to assess the risk of death from LUAD (22,23). The current study constructed a risk-scoring system based on 10 genes and classified patients into two different risk groups, and patients at higher risk was also found to have a worse prognosis, indicating that all 10 could be used as powerful markers for prognosis prediction in LUAD. Based on multifactorial COX proportional risk regression analysis, we further screened for three independent prognostic factors for LUAD: LDHA, TRIP13, and TTK, whose upregulated expression showed poorer survival, and these three genes were identified as important mRNAs affecting LUAD pro-

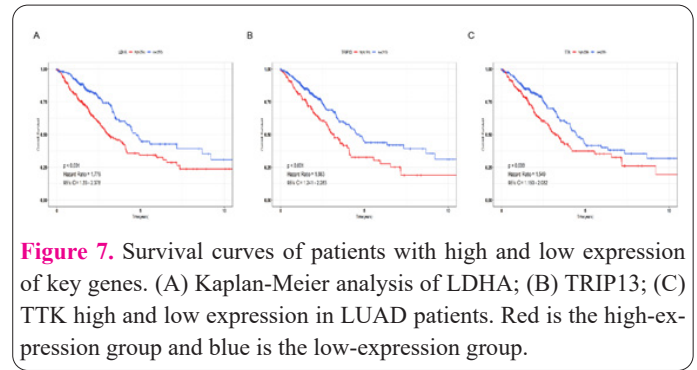


Figure 7. Survival curves of patients with high and low expression of key genes. (A) Kaplan-Meier analysis of LDHA; (B) TRIP13; (C) TTK high and low expression in LUAD patients. Red is the high-expression group and blue is the low-expression group.

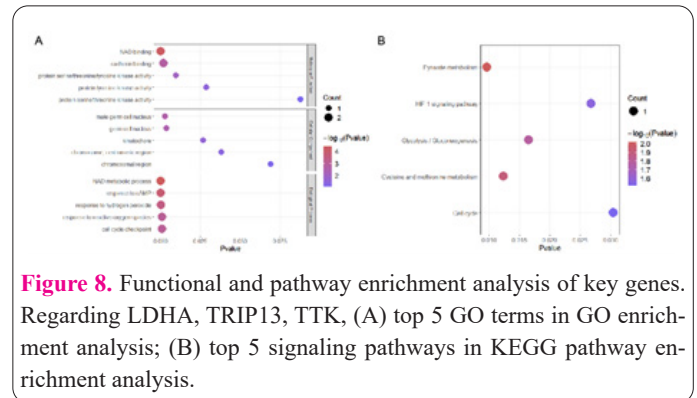


Figure 8. Functional and pathway enrichment analysis of key genes. Regarding LDHA, TRIP13, TTK, (A) top 5 GO terms in GO enrichment analysis; (B) top 5 signaling pathways in KEGG pathway enrichment analysis.

gnosis. NAD metabolism, cAMP, and other cancer-related processes are involved in cancer development (24-26).

LDHA is considered an ideal target in cancer therapy due to its indisputable role in the Warburg effect (27). It was shown that silencing LDHA does not induce apoptosis or autophagy through the mitochondrial pathway, despite the fact that LDHA exhibits similar high expression levels in prevalent tumor cells (28). However, its phosphorylation-mediated LDHA activation enhances the invasive potential of cancer cells and promotes tumor metastasis (28). Yu (29) et al. Have already found in their study that LDHA expression is upregulated in non-small cell lung cancer tissues and can act as an independent prognostic factor to predict overall and recurrence-free survival in LUAD. Encouragingly, LDHA-targeted inhibitors with anti-proliferative activity for lung cancer cells have been identified (30), providing strong support for their use as molecular targets for LUAD. In contrast, overexpression of TRIP13 and TTK has also been shown to be closely associated with malignant progression and poor prognosis of LUAD (31,32).

TRIP13 may be overexpressed in cancer cells in various forms, affecting the mitotic process of cells, leading to tumorigenesis and promoting the malignant transformation of cancer cells (33,34). TTK, on the other hand, is considered a potential therapeutic target and biological marker for lung cancer, and upregulation of TTK protein expression implies a more advanced lung cancer stage as well as poorer survival (35,36).

In conclusion, we in this study constructed co-expression networks and identified pivotal genes associated with LUAD by identifying DEGs in the LUAD expression profile in the TCGA database. This study provides a solid theoretical basis for the targeted treatment of LUAD, but further validation of this study is needed in future in vivo and ex vivo experiments, which will be the main direction of our subsequent research. This will also be the main direction of our subsequent research.

Conflict of interests

The authors declared no conflict of interest.

Funding

This study was funded by the (National Natural Science Foundation of China) (Grant number (81800805), (Qingdao Key Research Project) (Grant numbers (No. 17-3-3-10-nsh) and (19-6-1-3-nsh)) and (Qingdao Key Health Discipline Development Fund).

References

- Thandra KC, Barsouk A, Saginala K, Aluru JS, Barsouk A. Epidemiology of lung cancer. *Wspolczesna Onkol* 2021; 25(1): 45-52.
- Casal-Mourino A, Ruano-Ravina A, Lorenzo-Gonzalez M, et al. Epidemiology of stage III lung cancer: frequency, diagnostic characteristics, and survival. *Transl Lung Cancer R* 2021; 10(1): 506-518.
- Gonzalez MS, Motsch E, Trotter A, et al. Overdiagnosis in lung cancer screening: Estimates from the German Lung Cancer Screening Intervention Trial. *Int J Cancer* 2021; 148(5): 1097-1105.
- Suarez AA, Testoni B, Baumert TF, Lupberger J. Nucleic Acid-Induced Signaling in Chronic Viral Liver Disease. *Front Immunol* 2020; 11: 624034
- Calvayrac O, Pradines A, Pons E, Mazieres J, Guibert N. Molecular biomarkers for lung adenocarcinoma. *Eur Respir J* 2017; 49(4): 1601734.
- Yang X, Kui L, Tang M, et al. High-Throughput Transcriptome Profiling in Drug and Biomarker Discovery. *Front Genet* 2020; 11: 19.
- Hutter C, Zenklusen JC. The Cancer Genome Atlas: Creating Lasting Value beyond Its Data. *Cell* 2018; 173(2): 283-285.
- Sanchez-Vega F, Mina M, Armenia J, et al. Oncogenic Signaling Pathways in The Cancer Genome Atlas. *Cell* 2018; 173(2): 321-337.
- Shaikh D, Zhou Q, Chen T, Ibe JC, Raj JU, Zhou G. cAMP-dependent protein kinase is essential for hypoxia-mediated epithelial-mesenchymal transition, migration, and invasion in lung cancer cells. *Cell Signal* 2012; 24(12): 2396-2406.
- Piotrowski-Daspit AS, Nerger BA, Wolf AE, Sundaresan S, Nelson CM. Dynamics of Tissue-Induced Alignment of Fibrous Extracellular Matrix. *Biophys J* 2017; 113(3): 702-713.
- Jang M, Koh I, Lee JE, Lim JY, Cheong JH, Kim P. Increased extracellular matrix density disrupts E-cadherin/beta-catenin complex in gastric cancer cells. *Biomater Sci-Uk* 2018; 6(10): 2704-2713.
- Sapio L, Gallo M, Illiano M, et al. The Natural cAMP Elevating Compound Forskolin in Cancer Therapy: Is It Time? *J Cell Physiol* 2017; 232(5): 922-927.
- Alexeyenko A, Lee W, Pernemalm M, et al. Network enrichment analysis: extension of gene-set enrichment analysis to gene networks. *Bmc Bioinformatics* 2012; 13: 226.
- Liu P, Lu Z, Liu L, et al. NOD-like receptor signaling in inflammation-associated cancers: From functions to targeted therapies. *Phytomedicine* 2019; 64: 152925.
- Saxena M, Yeretssian G. NOD-Like Receptors: Master Regulators of Inflammation and Cancer. *Front Immunol* 2014; 5: 327.
- Cen X, Liu S, Cheng K. The Role of Toll-Like Receptor in Inflammation and Tumor Immunity. *Front Pharmacol* 2018; 9: 878.
- Moradi-Marjaneh R, Hassanian SM, Fiuji H, et al. Toll like receptor signaling pathway as a potential therapeutic target in colorectal cancer. *J Cell Physiol* 2018; 233(8): 5613-5622.
- Zhang B, Horvath S. A general framework for weighted gene co-expression network analysis. *Stat Appl Genet Mol* 2005; 4: Article17.
- Langfelder P, Horvath S. WGCNA: an R package for weighted correlation network analysis. *Bmc Bioinformatics* 2008; 9: 559.
- Yin L, Cai Z, Zhu B, Xu C. Identification of Key Pathways and Genes in the Dynamic Progression of HCC Based on WGCNA. *Genes-Basel* 2018; 9(2): 92.
- Xia WX, Yu Q, Li GH, et al. Identification of four hub genes associated with adrenocortical carcinoma progression by WGCNA. *Peerj* 2019; 7: e6555.
- Tang Z, Shen Y, Zhang X, Yi N. The spike-and-slab lasso Cox model for survival prediction and associated genes detection. *Bioinformatics* 2017; 33(18): 2799-2807.
- Wang W, Liu W. Integration of gene interaction information into a reweighted Lasso-Cox model for accurate survival prediction. *Bioinformatics* 2021; 36(22-23): 5405-5414.
- Yaku K, Okabe K, Hikosaka K, Nakagawa T. NAD Metabolism in Cancer Therapeutics. *Front Oncol* 2018; 8: 622.
- Chowdhry S, Zanca C, Rajkumar U, et al. NAD metabolic dependency in cancer is shaped by gene amplification and enhancer remodelling. *Nature* 2019; 569(7757): 570-575.
- Simko V, Iuliano F, Sevcikova A, et al. Hypoxia induces cancer-associated cAMP/PKA signalling through HIF-mediated transcriptional control of adenylyl cyclases VI and VII. *Sci Rep-Uk* 2017; 7(1): 10121.
- Pathria G, Scott DA, Feng Y, et al. Targeting the Warburg effect via LDHA inhibition engages ATF4 signaling for cancer cell survival. *Embo J* 2018; 37(20):
- Jin L, Chun J, Pan C, et al. Phosphorylation-mediated activation of LDHA promotes cancer cell invasion and tumour metastasis. *Oncogene* 2017; 36(27): 3797-3806.
- Yu C, Hou L, Cui H, et al. LDHA upregulation independently predicts poor survival in lung adenocarcinoma, but not in lung squamous cell carcinoma. *Future Oncol* 2018; 14(24): 2483-2492.
- Li XM, Xiao WH, Zhao HX. Discovery of potent human lactate dehydrogenase A (LDHA) inhibitors with antiproliferative activity against lung cancer cells: virtual screening and biological evaluation. *Medchemcomm* 2017; 8(3): 599-605.
- Li W, Zhang G, Li X, et al. Thyroid hormone receptor interactor 13 (TRIP13) overexpression associated with tumor progression and poor prognosis in lung adenocarcinoma. *Biochem Bioph Res Co* 2018; 499(3): 416-424.
- Da SCS, Dutra CB, Vidal GG, Lima-Maximino M, Pacheco RE, Maximino C. NOS-2 participates in the behavioral effects of ethanol withdrawal in zebrafish. *Neurosci Lett* 2020; 728: 134952.
- Lu S, Qian J, Guo M, Gu C, Yang Y. Insights into a Crucial Role of TRIP13 in Human Cancer. *Comput Struct Biotec* 2019; 17: 854-861.
- Li ZH, Lei L, Fei LR, et al. TRIP13 promotes the proliferation and invasion of lung cancer cells via the Wnt signaling pathway and epithelial-mesenchymal transition. *J Mol Histol* 2021; 52(1): 11-20.
- Chen X, Yu C, Gao J, et al. A novel USP9X substrate TTK contributes to tumorigenesis in non-small-cell lung cancer. *Theranostics* 2018; 8(9): 2348-2360.
- Chen J, Wu R, Xuan Y, Jiang M, Zeng Y. Bioinformatics analysis and experimental validation of TTK as a biomarker for prognosis in non-small cell lung cancer. *Bioscience Rep* 2020; 40(10): BSR20202711.